NASA TECHNICAL MEMORANDUM

NASA TM X-53641

July 31, 1967

NASA TM X-53641

AN ANALYSIS OF THE MOLECULAR KINETICS OF THE THERMOSPHERE PROBE

by James O. Ballance
Aero-Astrodynamics Laboratory

NASA

George C. Marshall Space Flight Center, Huntsville, Alabama

TECHNICAL MEMORANDUM X-53641

AN ANALYSIS OF THE MOLECULAR KINETICS OF THE THERMOSPHERE PROBE

By

James O. Ballance

George C. Marshall Space Flight Center

Huntsville, Alabama

ABSTRACT

A Monte Carlo computer analysis of the free molecular flow characteristics of the thermosphere probe used to measure gas temperature and density in the altitude range of 140 kilometers to 350 kilometers is described. The transmission probability which is required to relate the ambient density to the measured density is calculated for a simplified geometric configuration which compares well with measured signals except at high angles of attack where the simplified model of the system fails. The time response of the system seems to be adequate for the mode of measurements, and comparison with measured signals indicates that the incoming molecules made no more than 1 specular reflection if, indeed, any at all.

NASA - GEORGE C. MARSHALL SPACE FLIGHT CENTER

NASA - GEORGE C. MARSHALL SPACE FLIGHT CENTER

Technical Memorandum X-53641

AN ANALYSIS OF THE MOLECULAR KINETICS OF THE THERMOSPHERE PROBE

By

James O. Ballançe

AEROPHYSICS DIVISION
AERO-ASTRODYNAMICS LABORATORY
RESEARCH AND DEVELOPMENT OPERATIONS

TABLE OF CONTENTS

DEFINITION OF SYMBOLS

Symbol	Definition
$F(S)$	$e^{-S^2} - \sqrt{\pi}\, S[1 - ERF(S)]$
A	ratios of duct
k	Boltzmann's constant
m	mass of molecule
$\bar{V}$	average speed of molecule
V_m	most probable speed of molecule
N	number density of molecules
T	absolute temperature
U	free stream velocity
α	angle of attack
S	speed ratio, U/V_m
L	length of duct
K	Clausing probability factor (transmission probability)
Z	number of molecules
P	pressure
A_o	area of entrance orifice
A_i	area of exit orifice
TP	thermosphere probe

AN ANALYSIS OF THE MOLECULAR KINETICS OF THE THERMOSPHERE PROBE

SUMMARY

A Monte Carlo computer analysis of the free molecular flow characteristics of the thermosphere probe used to measure gas temperature and density in the altitude range of 140 kilometers to 350 kilometers is described. The transmission probability which is required to relate the ambient density to the measured density is calculated for a simplified geometric configuration which compares well with measured signals except at high angles of attack where the simplified model of the system fails. The time response of the system seems to be adequate for the mode of measurements, and comparison with measured signals indicates that the incoming molecules made no more than 1 specular reflection if, indeed, any at all.

I. INTRODUCTION

The thermosphere probe (TP) is an ejectable, sounding-rocket-borne system developed by the Space Physics Research Laboratory, Department of Electrical Engineering, University of Michigan, which makes simultaneous direct measurements of gas temperature and density, ion and electron density, and electron temperature in the earth's atmosphere in the altitude range from 120 km to 350 km. Among the complement of instruments used in this probe is an omegatron partial pressure gauge. A very critical area in the analysis of the data from this instrument is attenuation of the measured signal due to the velocity of the probe and the duct coupling the sensing region to the atmosphere. Previous theoretical approaches deviated from measured responses by as much as 20 percent [1]. This report describes a Monte Carlo analysis of the system, presents the results of this analysis, and compares these results with actual flight data.

II. DESCRIPTION OF THE OMEGATRON

The TP is a cylindrical probe approximately 32 inches long and 6 inches in diameter. The omegatron is located at one end of the cylinder with a circular duct protruding along the axis. A break-off device covers this duct and seals the system until operating altitudes are attained. Ignoring all details external to the probe cavity, figure 1 presents the internal duct configuration for the omegatron sensor showing the location of the sensing element. Basically, this cylindrical duct is 1 inch in diameter and approximately 1 7/16 inches long with a .438-inch diameter orifice connected to a rectangular duct about 3 3/4 inches long with sides of 1 inch and 1.312 inches. The omegatron sensing element is a cubic configuration approximately .688 inch on each edge having its center located along the axis of the cylindrical about 4 inches from the orifice. The detailed description of this sensor is not necessary for this analysis; however, an important feature is that the side of the cube which faces toward the orifice is solid plate. (A complete description of the omegatron is found in reference 2.) Thus, molecules entering the orifice must travel down the duct and pass between the duct wall and the forward plate before they can enter the sensing volume. Only those molecules which pass into the cubic volume can be measured.

III. MODIFIED CONFIGURATION FOR ANALYSIS

While the exact configuration of the omegatron could be analyzed by coupling several Monte Carlo programs, it was felt that a modified configuration could be used to obtain data with sufficient accuracy using only one program. Accordingly, the following assumptions were made:

(a) The conical section of ducting at the orifice could be eliminated, and the orifice could be considered to be an ideal orifice in an infinitely thin plane.

(b) The entire duct could be considered to be a cylinder.

(c) The limiting parameter at the sensor is the face toward the orifice. This parameter could be characterized by considering a circular disc within the cylinder whose area is the same proportion to the cross-sectional area of the cylinder as the cubic face area is to the cross-sectional area of the rectangular duct.

With these assumptions, a configuration with the following parameters was used (figure 2):

(a) The ratio of the length of the cylinder, L, to the radius of the cylinder, A_1, $L/A_1 = 5.5$

(b) The ratio of the radius of the orifice, A_o, to the radius of the cylinder, A_1, $(A_o/A_1) = .438$.

(c) The ratio of the radius of the circular disc, A_D, to the radius of the cylinder, A_1, $(A_D/A_1) = .6$.

IV. COMPUTER RESULTS

A. General Remarks

Using the input values from section III above, a Monte Carlo analysis was made of this configuration for speed ratios of 0.5, 1.0, 1.5, 1.64, 2.0, 2.38, 2.5, 2.7, and 3.0 at angles of attack of 0°, 10°, 20°, 30°, 45°, 60°, 75°, 90°, and 105°. Each molecule was followed until it exited or until it made 150 collisions. If it had made 150 collisions and had not yet exited the system, it was discarded. Very few were discarded, never more than 5 out of each sample of 10,000. The limit of 150 collisions was merely an arbitrary limit.

The transmission probability, K, (the probability that a molecule entering the orifice will pass through the tube and enter the sensor volume) is required to relate the density measured in the sensor volume to the ambient density through which the probe is passing. Appendix A presents the equations for this relationship involving the transmission probability. K is not only a function of the geometry, the speed ratio, and the angle of attack, but is also a function of the type of reflection a molecule makes after colliding with the surface. For vacuum systems where the mass velocity of the gas is small in comparison with the mean thermal speed of the molecules, diffuse reflections are assumed. As the relative velocity increases, as in a rocket probe, this may not be true. Accordingly, this program was written so that the molecules could make some number of specular collisions and after that number the remaining collisions, until they exited, were diffuse. The notation used to identify this parameter is zero specular, which means all reflections are diffuse, 1 specular, meaning that the first collision was specular and all subsequent diffuse, 2 specular, meaning that the first two collisions were specular and all subsequent diffuse, etc. The results of changing the parameter are clearly identified.

In addition to transmission probability, some information can be obtained from the program concerning the time of passage from the orifice to the sensor. This was done by assuming that the molecules traveled at the relative mass velocity of the probe until they were diffusely reflected from the walls at which time they traveled at a speed representative of the temperature of the probe. While these results are certainly not exact, they should point out any major time response problem if one existed.

B. Transmission Probability in Diffuse Reflections

Figures 3 through 11 present the transmission probabilities for the modified thermosphere probe configuration as a function of the angle of attack for various speed ratios. The expected trend of decreasing values of K with increasing values of the angle of attack is evident. In these figures, it is noticeable that, as the speed ratio increases, the value of K goes through a minimum and rises again and that the minimum value shifts toward lower angles of attack as the speed ratio increases.

While this trend is not significant in its magnitude, it is not believed to be representative of the original probe response, because of the initial assumptions of considering the entrance orifice as a pure orifice in an infinitely thin disc thus ignoring the conical section that actually contributes significantly to the flow properties at high angles of attack. This is shown more fully in the comparison of the Monte Carlo results with flight data.

Figure 12 shows the transmission probability for speed radios of 1, 2, and 3 and illustrates a significant feature of all types of probes at angles of attack. There is a particular angle of attack at which the transmission probability is independent of the speed ratio. This angle is usually near 30°, and the value of the transmission probability at that angle is approximately the value for the configuration when S equals 0. For this configuration, the transmission probability for S equals 0 is 0.640 where, for figure 12, the common value for the three speed ratios is approximately 0.660.

C. Specular Reflections

Tables I, II, and III contain the results of a study of specular reflection effects on the value of the transmission probabilities or at speed ratios of 1, 2, and 2.7, respectively. There is little difference between the K values for no specular reflection and 1 specular reflection, but there is a significant difference when there are 2 or more specular reflections. Also, for 2 or more specular reflections, the largest value of the transmission probability does not occur at zero angle of attack where the largest value does occur for diffuse reflections.

D. Time Response

Figure 13 presents typical results of the study of the time response characteristics of the thermosphere probe. For all speed ratios it requires more than 10 to 20 milliseconds for those molecules entering the omegatron sensor to transverse the tube. Since in normal operation the thermosphere probes tumble with a period of approximately 2 seconds, this means that in 10 milliseconds the orifice has swept through an angle of only 2 degrees so that essentially instantaneous response can be assumed through the analysis.

V. COMPARISON WITH FLIGHT DATA

The difference between the measured response and the theoretical response for the thermosphere was shown in reference 1. This same type of comparison is shown in figure 14 using the theoretical values as determined by the Monte Carlo analysis. Here the ratio of the measured signal to the theoretically produced value is shown as a function of the angle of attack for various speed ratios. Diffuse reflections are assumed for these comparisons. It is apparent that the two agree with $\mp$ 2 percent for angles of attack up to 75 degrees where considerable deviation begins. As mentioned earlier, this is believed to be due to the deficiency of the model used in the program where the actual conical orifice structure was not simulated in the configuration.

Although the comparison in figure 14 seems to be adequate, the possibility that better, or at least as good, agreements could be obtained with the theoretical values considering specular reflection. Using the results in a speed ratio of 2.7, the signal values were compared with the theoretical values (see tables IV through XII). From this comparison, it may be concluded that most likely the molecules did not have more than 1 specular reflection, if any at all.

VI. CONCLUSIONS

This study shows that Monte Carlo analysis of a simplified probe configuration provides adequate information about the characteristics of the thermosphere probe until the angle of attack becomes large enough where certain geometrical features of the probe which were ignored in the mathematical model begin to contribute a large error. Also, this study shows that there should be no major problems in the response time of the probe. Although a single specular reflection of the molecules may be possible, the analysis does show that more than 1 specular reflection does not appear to have occurred at these speed ratios.

TABLE 1

Transmission Probabilities for the

Modified Thermosphere Probe Configuration

Speed Ratio = 1.0

Number of Specular Reflections

Angle Of Attack	0	1	2	3	4	5	10
0	.669	.674	.766	.792	.751	.758	.754
10	.668	.677	.762	.790	.753	.748	.747
20	.672	.661	.766	.791	.762	.762	.756
30	.665	.657	.761	.790	.755	.757	.752
45	.645	.648	.741	.787	.768	.763	.744
60	.631	.639	.728	.774	.778	.779	.734
75	.632	.621	.720	.764	.785	.795	.751
90	.621	.625	.691	.747	.771	.783	.765
105	.620	.611	.672	.707	.741	.767	.761

TABLE II

Transmission Probabilities for the
Modified Thermosphere Probe Configuration

Speed Ratio = 2.0

Number of Specular Reflections

Angle Of Attack	0	1	2	3	4	5	6	8	10
0	.706	.712	.798	.819	.755	.765	.764	.766	.755
10	.719	.707	.802	.816	.763	.764	.765	.764	.753
20	.682	.688	.792	.805	.757	.767	.762	.755	.756
30	.663	.663	.773	.805	.770	.772	.765	.753	.748
45	.628	.624	.713	.769	.778	.768	.758	.746	.763
60	.607	.607	.688	.749	.761	.770	.759	.744	.749
75	.609	.609	.664	.717	.761	.777	.777	.773	.750
90	.598	.602	.643	.675	.723	.748	.774	.779	.779
105	.610	.604	.622	.652	.673	.704	.709	.739	.750

TABLE III

Transmission Probabilities for the Modified Thermosphere Probe Configuration

Speed Ratio = 2.7

Number of Specular Reflections

Angle Of Attack	0	1	2	3	4	5	6	8	10
0	.738	.747	.827	.831	.769	.762	.733	.762	.755
10	.732	.727	.831	.827	.776	.767	.763	.763	.749
20	.690	.694	.811	.826	.763	.765	.760	.743	.741
30	.656	.656	.780	.819	.780	.772	.760	.749	.745
45	.621	.618	.719	.779	.794	.794	.769	.755	.751
60	.604	.603	.614	.731	.763	.757	.771	.779	.746
90	.593	.542	.612	.657	.692	.718	.745	.772	.784
105	.612	.618	.606	.624	.646	.668	.686	.701	.726

TABLE IV

```
CALCULATION OF THE NORMALIZED RESPONSE CHARACTERISTICS OF THE
MUMP PROBE WITH MONTE CARLO VALUES FOR F(S) AND SPECULAR REFLECTIONS

SPEED RATIO =     2.7000
NUMBER OF SPECULAR REFLECTIONS =    0

ANGLE =   0.0   F(S) =  0.9571291E+01   F(S)*K =  0.1107149E+02
ANGLE =  10.0   F(S) =  0.9425892E+01   F(S)*K =  0.1081466E+02
ANGLE =  20.0   F(S) =  0.8994137E+01   F(S)*K =  0.9727201E+01
ANGLE =  30.0   F(S) =  0.8299257E+01   F(S)*K =  0.8523123E+01
ANGLE =  45.0   F(S) =  0.6770554E+01   F(S)*K =  0.6590147E+01
ANGLE =  60.0   F(S) =  0.4812680E+01   F(S)*K =  0.4556205E+01
ANGLE =  75.0   F(S) =  0.2690770E+01   F(S)*K =  0.2526287E+01
ANGLE =  90.0   F(S) =  0.9999996       F(S)*K =  0.9294667
ANGLE = 105.0   F(S) =  0.2157461       F(S)*K =  0.2069539

ANGLE =   0.0   NORM   F(S)*K = 1.000   SIGNAL TO F(S) RATIO =   1.000
ANGLE =  10.0   NORM   F(S)*K =  .977   SIGNAL TO F(S) RATIO =    .998
ANGLE =  20.0   NORM   F(S)*K =  .879   SIGNAL TO F(S) RATIO =   1.019
ANGLE =  30.0   NORM   F(S)*K =  .770   SIGNAL TO F(S) RATIO =   1.013
ANGLE =  45.0   NORM   F(S)*K =  .595   SIGNAL TO F(S) RATIO =   1.010
ANGLE =  60.0   NORM   F(S)*K =  .412   SIGNAL TO F(S) RATIO =   1.006
ANGLE =  75.0   NORM   F(S)*K =  .228   SIGNAL TO F(S) RATIO =   1.012
ANGLE =  90.0   NORM   F(S)*K =  .084   SIGNAL TO F(S) RATIO =   1.072
ANGLE = 105.0   NORM   F(S)*K =  .019   SIGNAL TO F(S) RATIO =   1.070
```

TABLE V

CALCULATION OF THE NORMALIZED RESPONSE CHARACTERISTICS OF THE MUMP PROBE WITH MONTE CARLO VALUES FOR F(S) AND SPECULAR REFLECTIONS

SPEED RATIO = 2.7000
NUMBER OF SPECULAR REFLECTIONS = 1

ANGLE	=	0.0	F(S)	=	0.9571291E+01	F(S)*K =	0.1120801E+02
ANGLE	=	10.0	F(S)	=	0.9425892E+01	F(S)*K =	0.1073636E+02
ANGLE	=	20.0	F(S)	=	0.8994137E+01	F(S)*K =	0.9777952E+01
ANGLE	=	30.0	F(S)	=	0.8289257E+01	F(S)*K =	0.8519226E+01
ANGLE	=	45.0	F(S)	=	0.6770554E+01	F(S)*K =	0.6553005E+01
ANGLE	=	60.0	F(S)	=	0.4812680E+01	F(S)*K =	0.4550170E+01
ANGLE	=	75.0	F(S)	=	0.2690770E+01	F(S)*K =	0.2531770E+01
ANGLE	=	90.0	F(S)	=	0.9999996	F(S)*K =	0.9282128
ANGLE	=	105.0	F(S)	=	0.2157461	F(S)*K =	0.2090505

ANGLE	=	0.0	NORM F(S)*K =	1.000	SIGNAL TO F(S) RATIO =	1.000
ANGLE	=	10.0	NORM F(S)*K =	.958	SIGNAL TO F(S) RATIO =	1.018
ANGLE	=	20.0	NORM F(S)*K =	.872	SIGNAL TO F(S) RATIO =	1.026
ANGLE	=	30.0	NORM F(S)*K =	.760	SIGNAL TO F(S) RATIO =	1.026
ANGLE	=	45.0	NORM F(S)*K =	.585	SIGNAL TO F(S) RATIO =	1.028
ANGLE	=	60.0	NORM F(S)*K =	.406	SIGNAL TO F(S) RATIO =	1.020
ANGLE	=	75.0	NORM F(S)*K =	.226	SIGNAL TO F(S) RATIO =	1.023
ANGLE	=	90.0	NORM F(S)*K =	.083	SIGNAL TO F(S) RATIO =	1.087
ANGLE	=	105.0	NORM F(S)*K =	.019	SIGNAL TO F(S) RATIO =	1.072

TABLE VI

CALCULATION OF THE NORMALIZED RESPONSE CHARACTERISTICS OF THE MUMP PROBE WITH MONTE CARLO VALUES FOR F(S) AND SPECULAR REFLECTIONS

SPEED RATIO = 2.7000

NUMBER OF SPECULAR REFLECTIONS = 2

ANGLE	F(S)	F(S)*K
0.0	0.9571291E+01	0.1240967E+02
10.0	0.9425892E+01	0.1226991E+02
20.0	0.8994137E+01	0.1143722E+02
30.0	0.8289257E+01	0.1013810E+02
45.0	0.6770554E+01	0.7624832E+01
60.0	0.4812680E+01	0.4932620E+01
75.0	0.2690770E+01	0.2699626E+01
90.0	0.9999996	0.9589338
105.0	0.2157461	0.2048235

ANGLE	NORM F(S)*K	SIGNAL TO F(S) RATIO
0.0	1.000	1.000
10.0	.989	.986
20.0	.922	.971
30.0	.817	.955
45.0	.614	.978
60.0	.397	1.042
75.0	.218	1.062
90.0	.077	1.165
105.0	.017	1.212

TABLE VII

```
CALCULATION OF THE NORMALIZED RESPONSE CHARACTERISTICS OF THE
MUMP PROBE WITH MONTE CARLO VALUES FOR F(S) AND SPECULAR REFLECTIONS

SPEED RATIO =     2.7000
NUMBER OF SPECULAR REFLECTIONS =   3

ANGLE =   0.0  F(S) =  0.9571291E+01  F(S)*K =  0.1245918E+02
ANGLE =  10.0  F(S) =  0.9425892E+01  F(S)*K =  0.1221968E+02
ANGLE =  20.0  F(S) =  0.8994137E+01  F(S)*K =  0.1164727E+02
ANGLE =  30.0  F(S) =  0.8289257E+01  F(S)*K =  0.1063442E+02
ANGLE =  45.0  F(S) =  0.6770554E+01  F(S)*K =  0.8265806E+01
ANGLE =  60.0  F(S) =  0.4812680E+01  F(S)*K =  0.5510443E+01
ANGLE =  75.0  F(S) =  0.2690770E+01  F(S)*K =  0.2920059E+01
ANGLE =  90.0  F(S) =  0.9999996      F(S)*K =  0.1030094E+01
ANGLE = 105.0  F(S) =  0.2157461      F(S)*K =  0.2111133

ANGLE =   0.0  NORM  F(S)*K = 1.000  SIGNAL TO F(S) RATIO =  1.000
ANGLE =  10.0  NORM  F(S)*K =  .981  SIGNAL TO F(S) RATIO =   .994
ANGLE =  20.0  NORM  F(S)*K =  .935  SIGNAL TO F(S) RATIO =   .957
ANGLE =  30.0  NORM  F(S)*K =  .854  SIGNAL TO F(S) RATIO =   .914
ANGLE =  45.0  NORM  F(S)*K =  .663  SIGNAL TO F(S) RATIO =   .906
ANGLE =  60.0  NORM  F(S)*K =  .442  SIGNAL TO F(S) RATIO =   .936
ANGLE =  75.0  NORM  F(S)*K =  .235  SIGNAL TO F(S) RATIO =   .983
ANGLE =  90.0  NORM  F(S)*K =  .083  SIGNAL TO F(S) RATIO =  1.080
ANGLE = 105.0  NORM  F(S)*K =  .017  SIGNAL TO F(S) RATIO =  1.180
```

TABLE VIII

```
CALCULATION OF THE NORMALIZED RESPONSE CHARACTERISTICS OF THE
MUMP PROBE WITH MONTE CARLO VALUES FOR F(S) AND SPECULAR REFLECTIONS

SPEED RATIO =     2.7000
NUMBER OF SPECULAR REFLECTIONS =   4

ANGLE =   0.0  F(S) =  0.9571291E+01  F(S)*K =  0.1152506E+02
ANGLE =  10.0  F(S) =  0.9425802E+01  F(S)*K =  0.1145881E+02
ANGLE =  20.0  F(S) =  0.8994137E+01  F(S)*K =  0.1074926E+02
ANGLE =  30.0  F(S) =  0.8289257E+01  F(S)*K =  0.1012771E+02
ANGLE =  45.0  F(S) =  0.6770554E+01  F(S)*K =  0.8427111E+01
ANGLE =  60.0  F(S) =  0.4812680E+01  F(S)*K =  0.5752585E+01
ANGLE =  75.0  F(S) =  0.2690770E+01  F(S)*K =  0.3104929E+01
ANGLE =  90.0  F(S) =  0.9999996      F(S)*K =  0.1084482E+01
ANGLE = 105.0  F(S) =  0.2157461      F(S)*K =  0.2183499

ANGLE =   0.0  NORM  F(S)*K = 1.000  SIGNAL TO F(S) RATIO =  1.000
ANGLE =  10.0  NORM  F(S)*K =  .993  SIGNAL TO F(S) RATIO =   .981
ANGLE =  20.0  NORM  F(S)*K =  .932  SIGNAL TO F(S) RATIO =   .960
ANGLE =  30.0  NORM  F(S)*K =  .878  SIGNAL TO F(S) RATIO =   .888
ANGLE =  45.0  NORM  F(S)*K =  .731  SIGNAL TO F(S) RATIO =   .823
ANGLE =  60.0  NORM  F(S)*K =  .499  SIGNAL TO F(S) RATIO =   .830
ANGLE =  75.0  NORM  F(S)*K =  .269  SIGNAL TO F(S) RATIO =   .858
ANGLE =  90.0  NORM  F(S)*K =  .094  SIGNAL TO F(S) RATIO =   .957
ANGLE = 105.0  NORM  F(S)*K =  .019  SIGNAL TO F(S) RATIO =  1.057
```

TABLE IX

CALCULATION OF THE NORMALIZED RESPONSE CHARACTERISTICS OF THE MUMP PROBE WITH MONTE CARLO VALUES FOR F(S) AND SPECULAR REFLECTIONS

SPEED RATIO = 2.7000
NUMBER OF SPECULAR REFLECTIONS = 5

ANGLE =	0.0	F(S) = 0.9571291E+01	F(S)*K = 0.1142404E+02
ANGLE =	10.0	F(S) = 0.9425892E+01	F(S)*K = 0.1133176E+02
ANGLE =	20.0	F(S) = 0.8994137E+01	F(S)*K = 0.1077887E+02
ANGLE =	30.0	F(S) = 0.8289257E+01	F(S)*K = 0.1002506E+02
ANGLE =	45.0	F(S) = 0.6770554E+01	F(S)*K = 0.8427111E+01
ANGLE =	60.0	F(S) = 0.4812680E+01	F(S)*K = 0.5869508E+01
ANGLE =	75.0	F(S) = 0.2690770E+01	F(S)*K = 0.3192653E+01
ANGLE =	90.0	F(S) = 0.9999996	F(S)*K = 0.1125235E+01
ANGLE =	105.0	F(S) = 0.2157461	F(S)*K = 0.2258571

ANGLE =	0.0	NORM F(S)*K = 1.000	SIGNAL TO F(S) RATIO = 1.000
ANGLE =	10.0	NORM F(S)*K = .992	SIGNAL TO F(S) RATIO = .983
ANGLE =	20.0	NORM F(S)*K = .944	SIGNAL TO F(S) RATIO = .949
ANGLE =	30.0	NORM F(S)*K = .878	SIGNAL TO F(S) RATIO = .889
ANGLE =	45.0	NORM F(S)*K = .738	SIGNAL TO F(S) RATIO = .815
ANGLE =	60.0	NORM F(S)*K = .514	SIGNAL TO F(S) RATIO = .806
ANGLE =	75.0	NORM F(S)*K = .279	SIGNAL TO F(S) RATIO = .827
ANGLE =	90.0	NORM F(S)*K = .098	SIGNAL TO F(S) RATIO = .914
ANGLE =	105.0	NORM F(S)*K = .020	SIGNAL TO F(S) RATIO = 1.012

TABLE X

CALCULATION OF THE NORMALIZED RESPONSE CHARACTERISTICS OF THE MUMP PROBE WITH MONTE CARLO VALUES FOR F(S) AND SPECULAR REFLECTIONS

SPEED RATIO = 2.7000
NUMBER OF SPECULAR REFLECTIONS = 6

ANGLE = 0.0	F(S) = 0.9571291E+01	F(S)*K = 0.1099648E+02
ANGLE = 10.0	F(S) = 0.9425892E+01	F(S)*K = 0.1127414E+02
ANGLE = 20.0	F(S) = 0.8994137E+01	F(S)*K = 0.1064071E+02
ANGLE = 30.0	F(S) = 0.8289257E+01	F(S)*K = 0.9878248E+01
ANGLE = 45.0	F(S) = 0.6770554E+01	F(S)*K = 0.8162869E+01
ANGLE = 60.0	F(S) = 0.4812680E+01	F(S)*K = 0.5788039E+01
ANGLE = 75.0	F(S) = 0.2690770E+01	F(S)*K = 0.3251276E+01
ANGLE = 90.0	F(S) = 0.9999996	F(S)*K = 0.1168338E+01
ANGLE = 105.0	F(S) = 0.2157461	F(S)*K = 0.2319439

ANGLE = 0.0	NORM F(S)*K = 1.000	SIGNAL TO F(S) RATIO = 1.000
ANGLE = 10.0	NORM F(S)*K = 1.025	SIGNAL TO F(S) RATIO = .951
ANGLE = 20.0	NORM F(S)*K = .968	SIGNAL TO F(S) RATIO = .925
ANGLE = 30.0	NORM F(S)*K = .898	SIGNAL TO F(S) RATIO = .868
ANGLE = 45.0	NORM F(S)*K = .742	SIGNAL TO F(S) RATIO = .810
ANGLE = 60.0	NORM F(S)*K = .526	SIGNAL TO F(S) RATIO = .787
ANGLE = 75.0	NORM F(S)*K = .296	SIGNAL TO F(S) RATIO = .781
ANGLE = 90.0	NORM F(S)*K = .106	SIGNAL TO F(S) RATIO = .847
ANGLE = 105.0	NORM F(S)*K = .021	SIGNAL TO F(S) RATIO = .948

TABLE XI

CALCULATION OF THE NORMALIZED RESPONSE CHARACTERISTICS OF THE MUMP PROBE WITH MONTE CARLO VALUES FOR F(S) AND SPECULAR REFLECTIONS

SPEED RATIO = 2.7000
NUMBER OF SPECULAR REFLECTIONS = 8

ANGLE =	0.0	F(S) =	0.9571291E+01	F(S)*K =	0.1143154E+02		
ANGLE =	10.0	F(S) =	0.9425892E+01	F(S)*K =	0.1126970E+02		
ANGLE =	20.0	F(S) =	0.8994137E+01	F(S)*K =	0.1046872E+02		
ANGLE =	30.0	F(S) =	0.8289257E+01	F(S)*K =	0.9736629E+01		
ANGLE =	45.0	F(S) =	0.6770554E+01	F(S)*K =	0.8011115E+01		
ANGLE =	60.0	F(S) =	0.4812680E+01	F(S)*K =	0.5625102E+01		
ANGLE =	75.0	F(S) =	0.2690770E+01	F(S)*K =	0.3283751E+01		
ANGLE =	90.0	F(S) =	0.9999996	F(S)*K =	0.1209561E+01		
ANGLE =	105.0	F(S) =	0.2157461	F(S)*K =	0.2369487		

ANGLE =	0.0	NORM F(S)*K =	1.000	SIGNAL TO F(S) RATIO =	1.000
ANGLE =	10.0	NORM F(S)*K =	.986	SIGNAL TO F(S) RATIO =	.989
ANGLE =	20.0	NORM F(S)*K =	.916	SIGNAL TO F(S) RATIO =	.977
ANGLE =	30.0	NORM F(S)*K =	.852	SIGNAL TO F(S) RATIO =	.916
ANGLE =	45.0	NORM F(S)*K =	.701	SIGNAL TO F(S) RATIO =	.858
ANGLE =	60.0	NORM F(S)*K =	.492	SIGNAL TO F(S) RATIO =	.841
ANGLE =	75.0	NORM F(S)*K =	.287	SIGNAL TO F(S) RATIO =	.804
ANGLE =	90.0	NORM F(S)*K =	.106	SIGNAL TO F(S) RATIO =	.851
ANGLE =	105.0	NORM F(S)*K =	.021	SIGNAL TO F(S) RATIO =	.965

TABLE XII

CALCULATION OF THE NORMALIZED RESPONSE CHARACTERISTICS OF THE MUMP PROBE WITH MONTE CARLO VALUES FOR F(S) AND SPECULAR REFLECTIONS

SPEED RATIO = 2.7000
NUMBER OF SPECULAR REFLECTIONS = 10

ANGLE =	0.0	F(S) =	0.9571291E+01	F(S)*K =	0.1133253E+02
ANGLE =	10.0	F(S) =	0.9425892E+01	F(S)*K =	0.1107173E+02
ANGLE =	20.0	F(S) =	0.8994137E+01	F(S)*K =	0.1044335E+02
ANGLE =	30.0	F(S) =	0.8289257E+01	F(S)*K =	0.9679462E+01
ANGLE =	45.0	F(S) =	0.6770554E+01	F(S)*K =	0.7971850E+01
ANGLE =	60.0	F(S) =	0.4812680E+01	F(S)*K =	0.5626611E+01
ANGLE =	75.0	F(S) =	0.2690770E+01	F(S)*K =	0.3145417E+01
ANGLE =	90.0	F(S) =	0.9999996	F(S)*K =	0.1228996E+01
ANGLE =	105.0	F(S) =	0.2157461	F(S)*K =	0.2454365

ANGLE =	0.0	NORM F(S)*K =	1.000	SIGNAL TO F(S) RATIO =	1.000
ANGLE =	10.0	NORM F(S)*K =	.977	SIGNAL TO F(S) RATIO =	.998
ANGLE =	20.0	NORM F(S)*K =	.922	SIGNAL TO F(S) RATIO =	.971
ANGLE =	30.0	NORM F(S)*K =	.854	SIGNAL TO F(S) RATIO =	.913
ANGLE =	45.0	NORM F(S)*K =	.703	SIGNAL TO F(S) RATIO =	.854
ANGLE =	60.0	NORM F(S)*K =	.497	SIGNAL TO F(S) RATIO =	.834
ANGLE =	75.0	NORM F(S)*K =	.278	SIGNAL TO F(S) RATIO =	.832
ANGLE =	90.0	NORM F(S)*K =	.108	SIGNAL TO F(S) RATIO =	.830
ANGLE =	105.0	NORM F(S)*K =	.022	SIGNAL TO F(S) RATIO =	.923

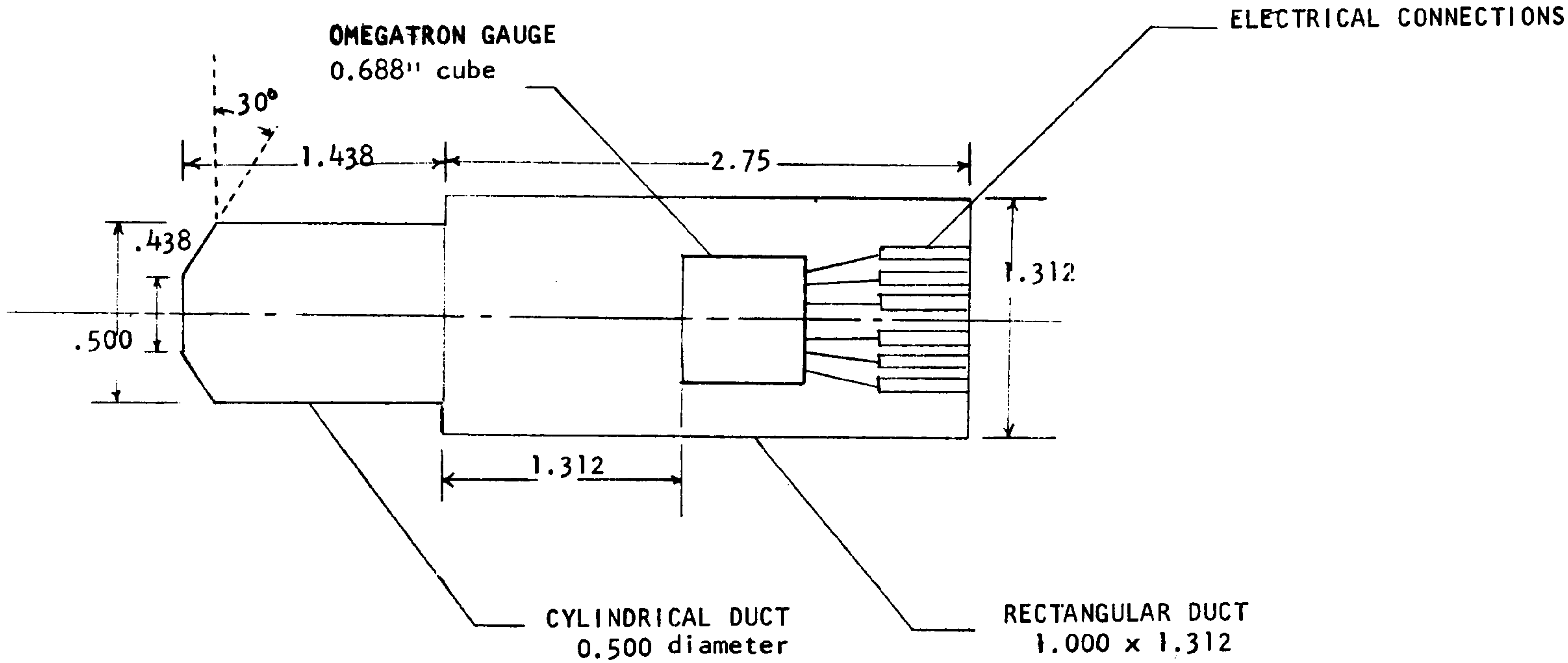

Figure 1. Internal Configuration for the Omegatron Thermosphere Probe

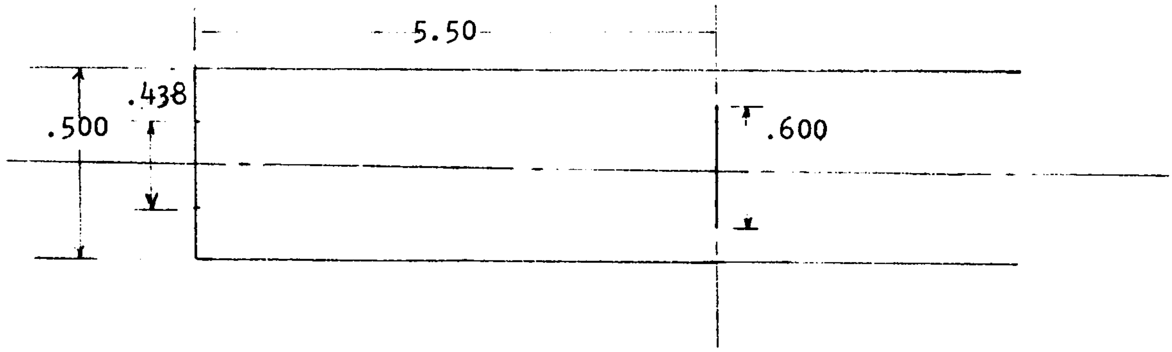

Figure 2. Modified Internal Configuration of the Omegatron for the Computer Analysis of Molecular Flow

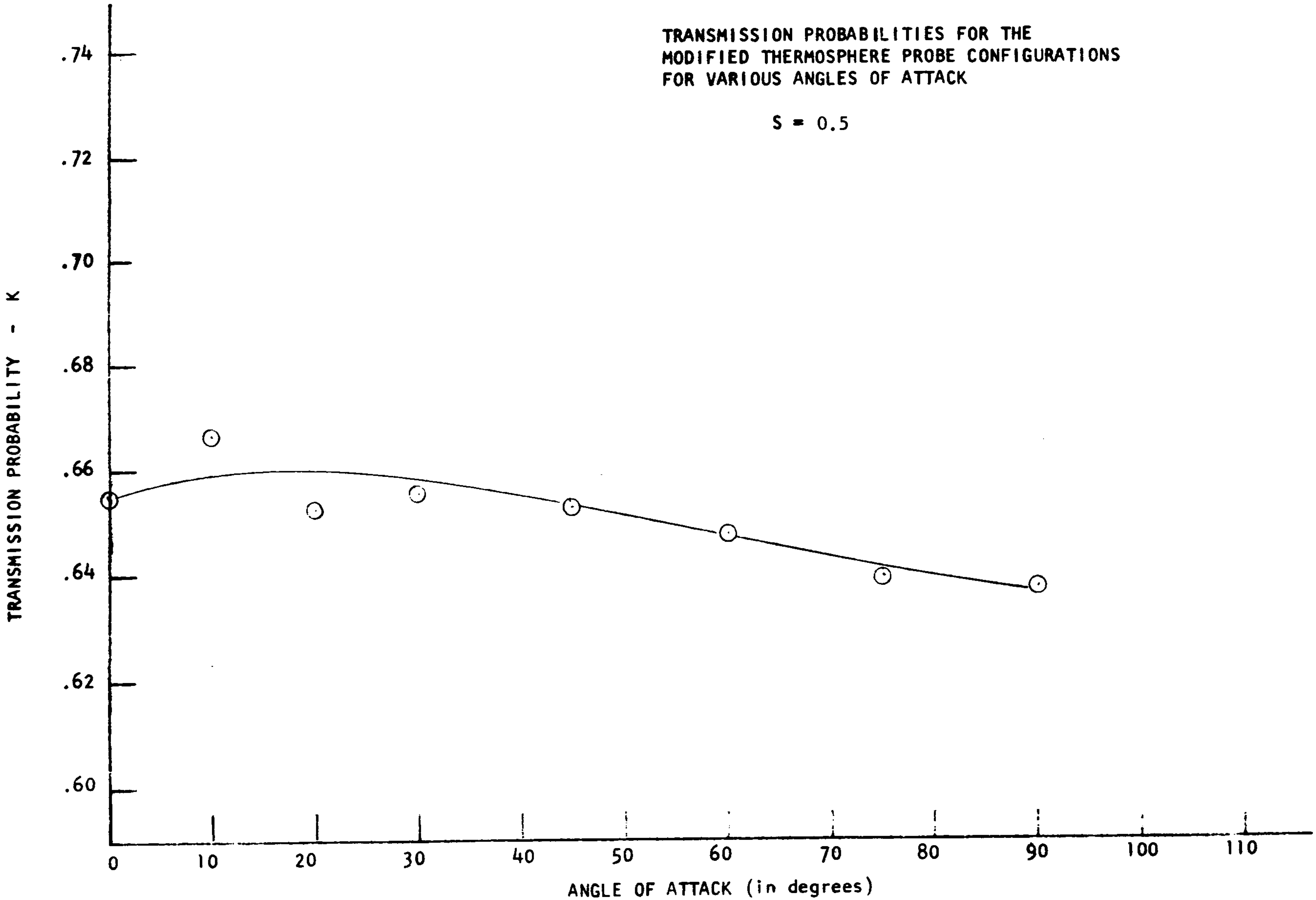
TRANSMISSION PROBABILITIES FOR THE
MODIFIED THERMOSPHERE PROBE CONFIGURATIONS
FOR VARIOUS ANGLES OF ATTACK
S = 0.5
TRANSMISSION PROBABILITY - K
.74
.72
.70
.68
.66
.64
.62
.60
0
10
20
30
40
50
60
70
80
90
100
110
ANGLE OF ATTACK (in degrees)

FIGURE 3

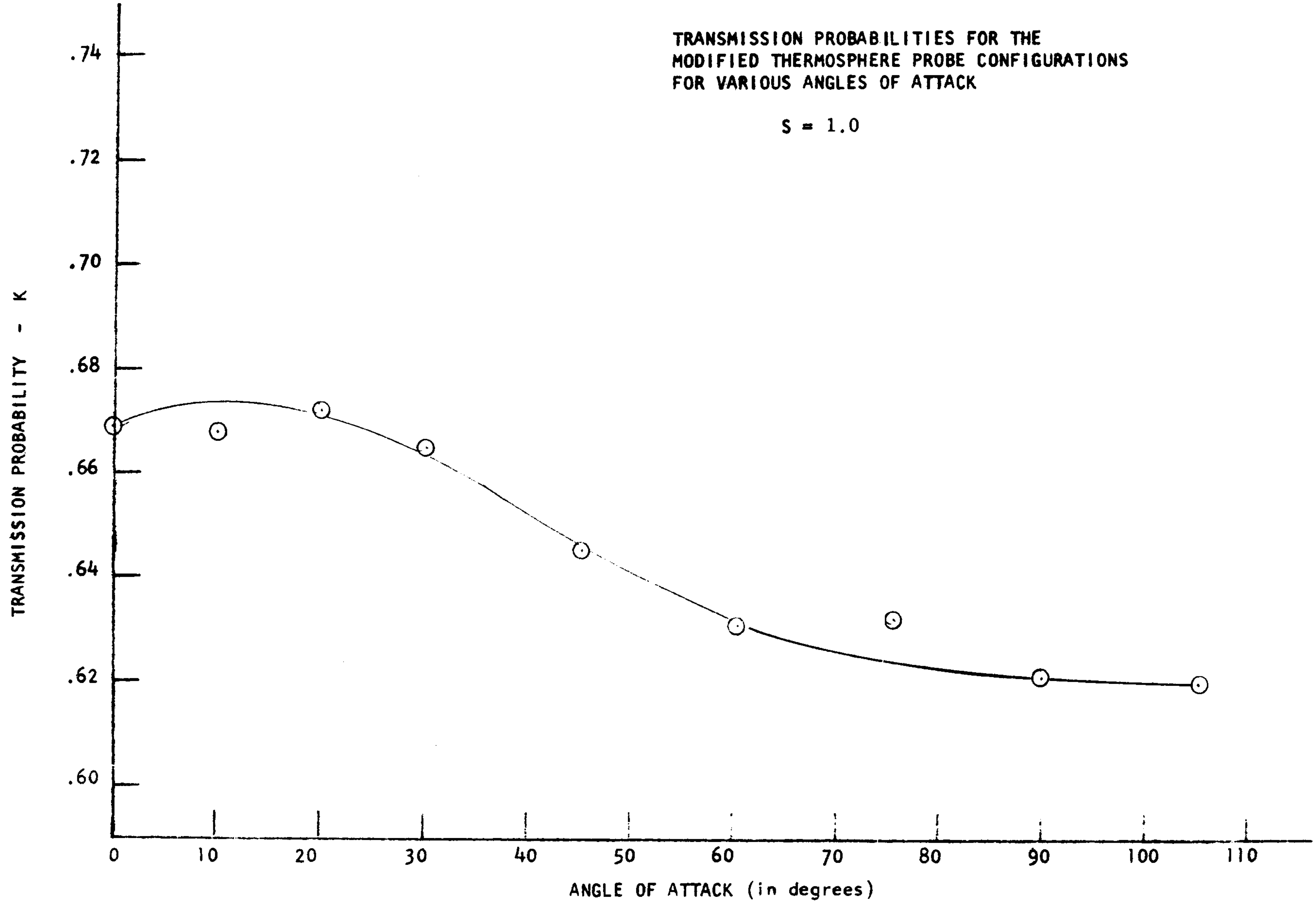
TRANSMISSION PROBABILITIES FOR THE
MODIFIED THERMOSPHERE PROBE CONFIGURATIONS
FOR VARIOUS ANGLES OF ATTACK
S = 1.0
TRANSMISSION PROBABILITY - K
.74
.72
.70
.68
.66
.64
.62
.60
0
10
20
30
40
50
60
70
80
90
100
110
ANGLE OF ATTACK (in degrees)

FIGURE 4

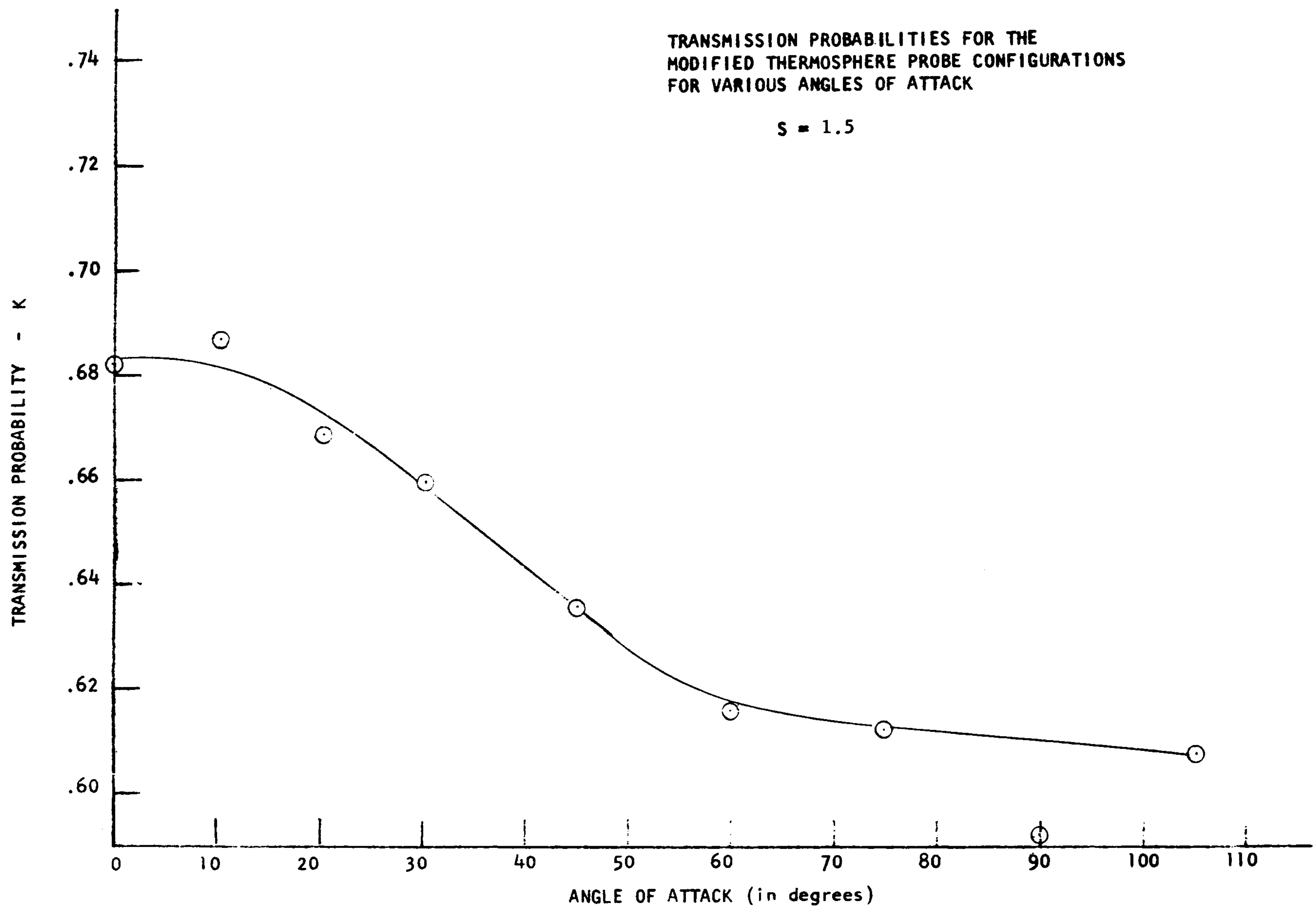
TRANSMISSION PROBABILITIES FOR THE
MODIFIED THERMOSPHERE PROBE CONFIGURATIONS
FOR VARIOUS ANGLES OF ATTACK
S = 1.5
TRANSMISSION PROBABILITY - K
.74
.72
.70
.68
.66
.64
.62
.60
0
10
20
30
40
50
60
70
80
90
100
110
ANGLE OF ATTACK (in degrees)

FIGURE 5

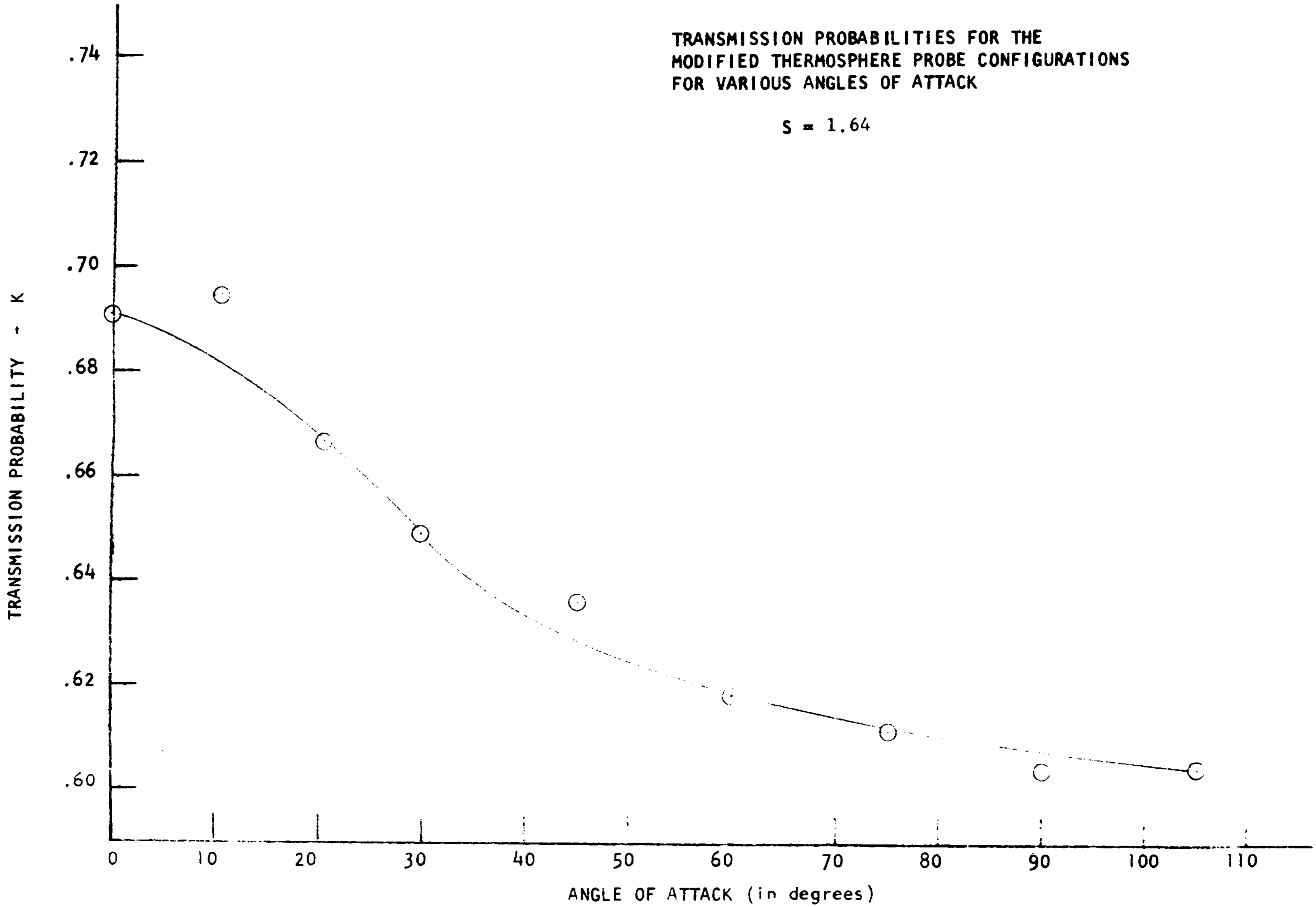

TRANSMISSION PROBABILITIES FOR THE
MODIFIED THERMOSPHERE PROBE CONFIGURATIONS
FOR VARIOUS ANGLES OF ATTACK
S = 1.64
TRANSMISSION PROBABILITY - K
.74
.72
.70
.68
.66
.64
.62
.60
0
10
20
30
40
50
60
70
80
90
100
110
ANGLE OF ATTACK (in degrees)

FIGURE 6

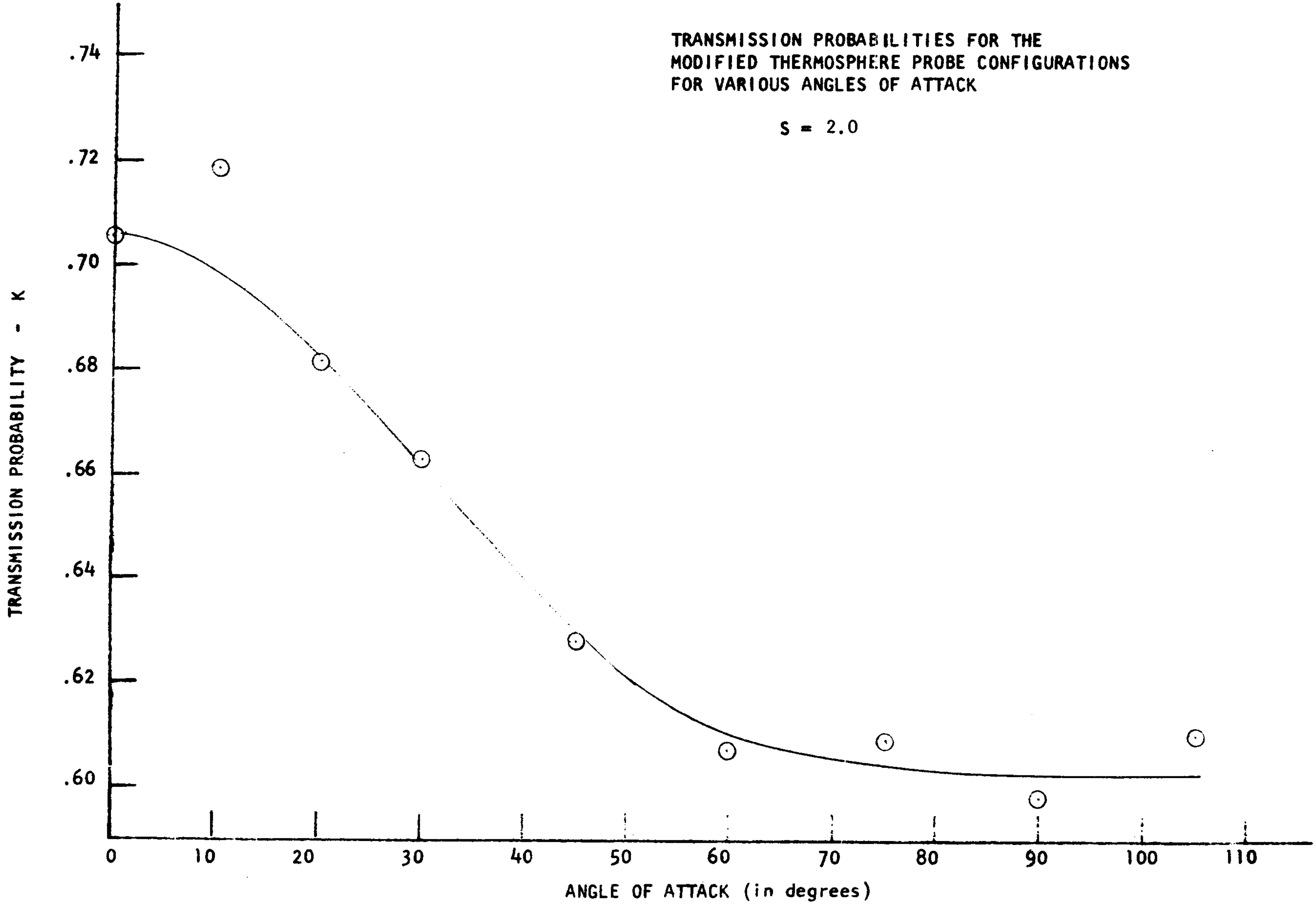
TRANSMISSION PROBABILITIES FOR THE
MODIFIED THERMOSPHERE PROBE CONFIGURATIONS
FOR VARIOUS ANGLES OF ATTACK
S = 2.0
TRANSMISSION PROBABILITY - K
.74
.72
.70
.68
.66
.64
.62
.60
0
10
20
30
40
50
60
70
80
90
100
110
ANGLE OF ATTACK (in degrees)

FIGURE 7

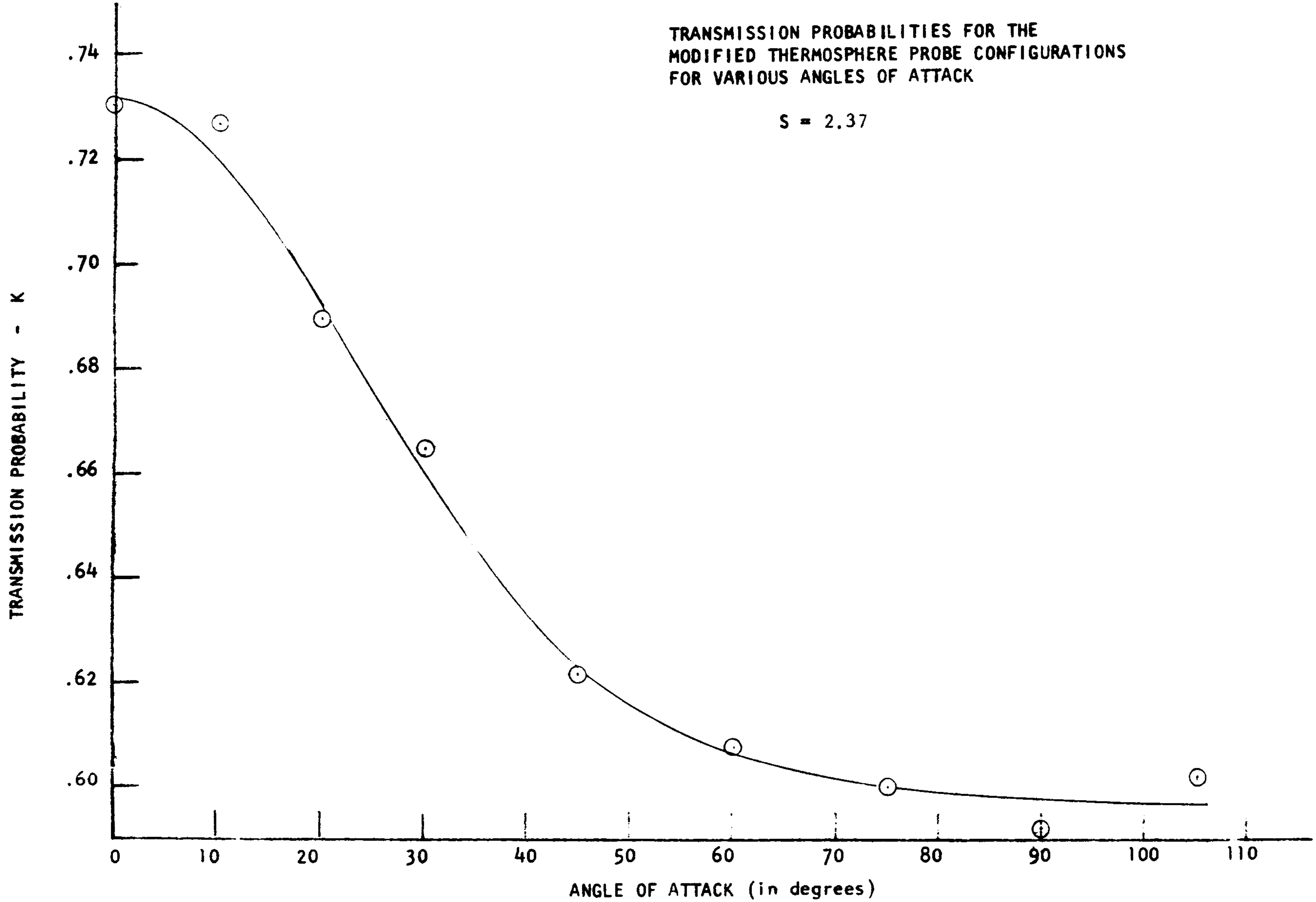
TRANSMISSION PROBABILITIES FOR THE
MODIFIED THERMOSPHERE PROBE CONFIGURATIONS
FOR VARIOUS ANGLES OF ATTACK
S = 2.37
TRANSMISSION PROBABILITY - K
.74
.72
.70
.68
.66
.64
.62
.60
0
10
20
30
40
50
60
70
80
90
100
110
ANGLE OF ATTACK (in degrees)

FIGURE 8

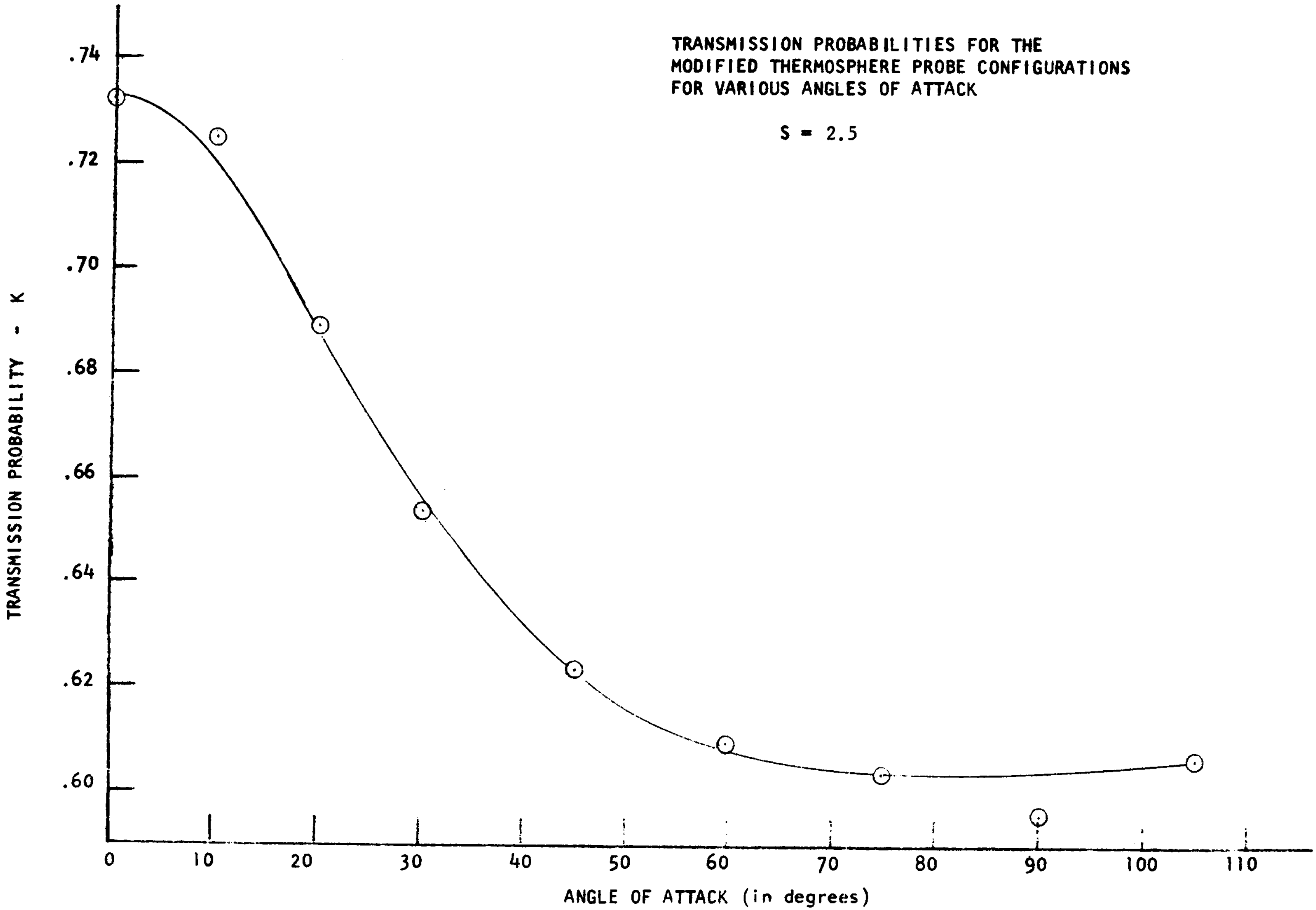
TRANSMISSION PROBABILITIES FOR THE
MODIFIED THERMOSPHERE PROBE CONFIGURATIONS
FOR VARIOUS ANGLES OF ATTACK
S = 2.5
TRANSMISSION PROBABILITY - K
.74
.72
.70
.68
.66
.64
.62
.60
0
10
20
30
40
50
60
70
80
90
100
110
ANGLE OF ATTACK (in degrees)

FIGURE 9

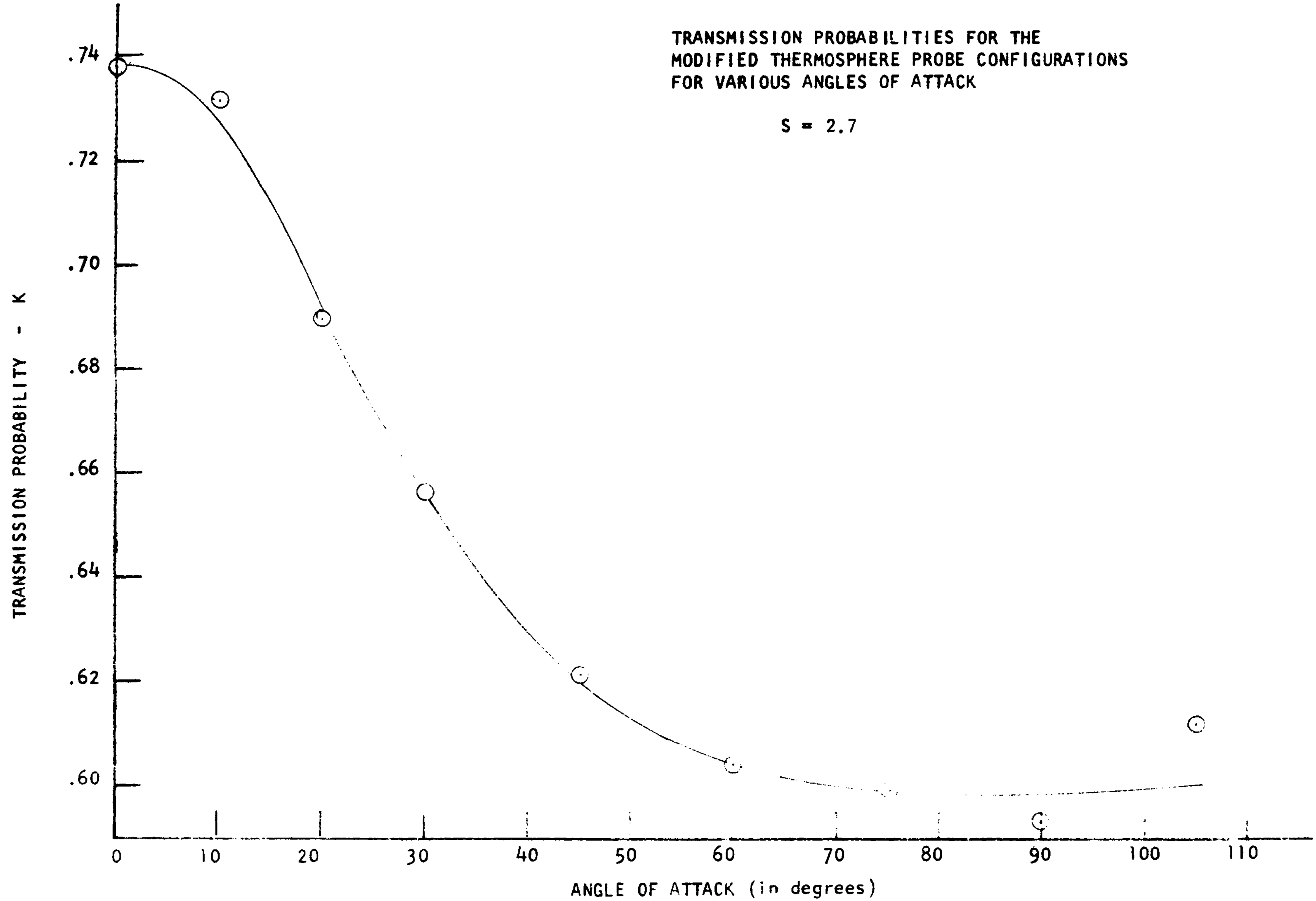
TRANSMISSION PROBABILITIES FOR THE
MODIFIED THERMOSPHERE PROBE CONFIGURATIONS
FOR VARIOUS ANGLES OF ATTACK
S = 2.7
TRANSMISSION PROBABILITY - K
.74
.72
.70
.68
.66
.64
.62
.60
0
10
20
30
40
50
60
70
80
90
100
110
ANGLE OF ATTACK (in degrees)

FIGURE 10

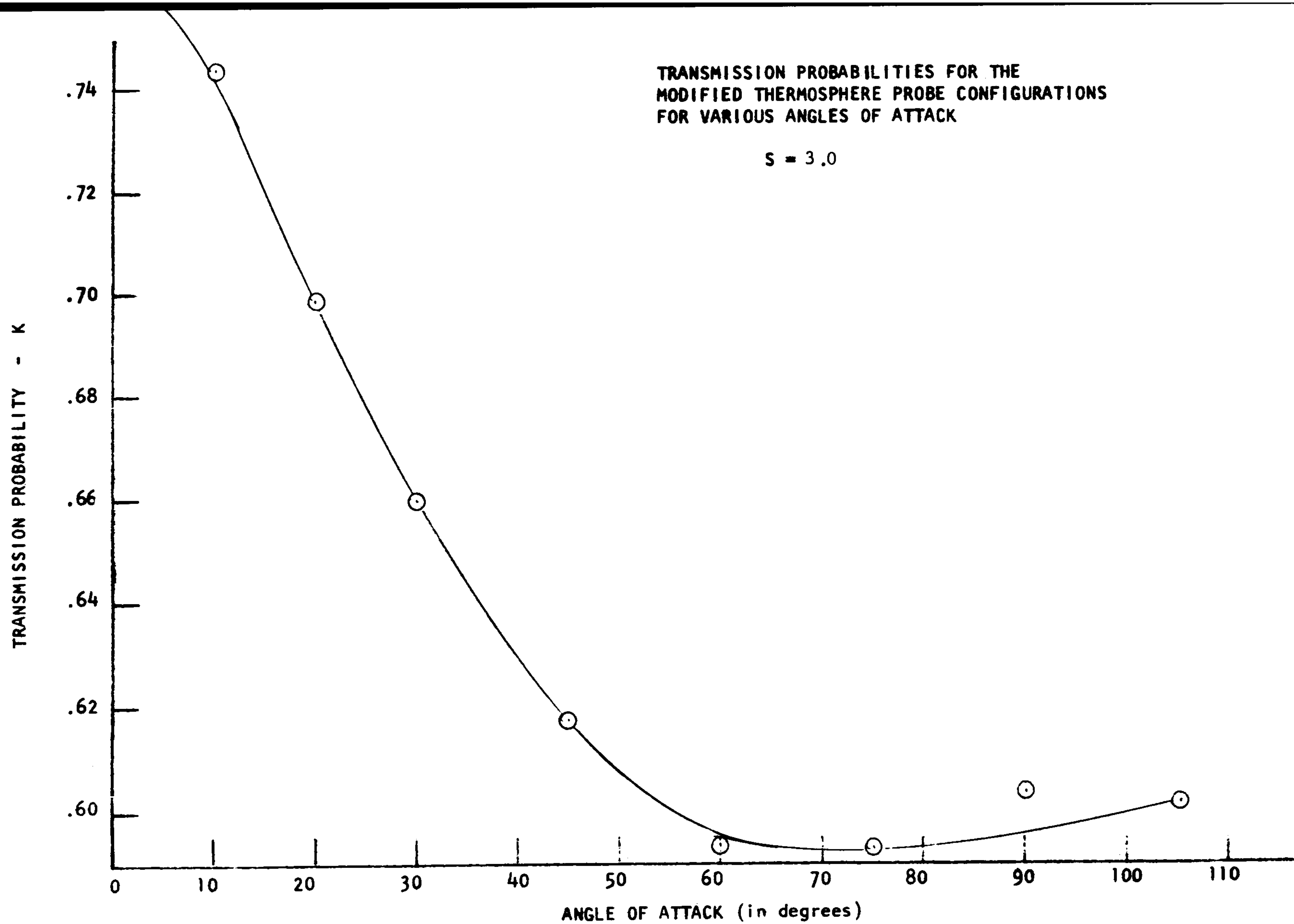
TRANSMISSION PROBABILITIES FOR THE
MODIFIED THERMOSPHERE PROBE CONFIGURATIONS
FOR VARIOUS ANGLES OF ATTACK
S = 3.0
TRANSMISSION PROBABILITY - K
.74
.72
.70
.68
.66
.64
.62
.60
0
10
20
30
40
50
60
70
80
90
100
110
ANGLE OF ATTACK (in degrees)

FIGURE 11

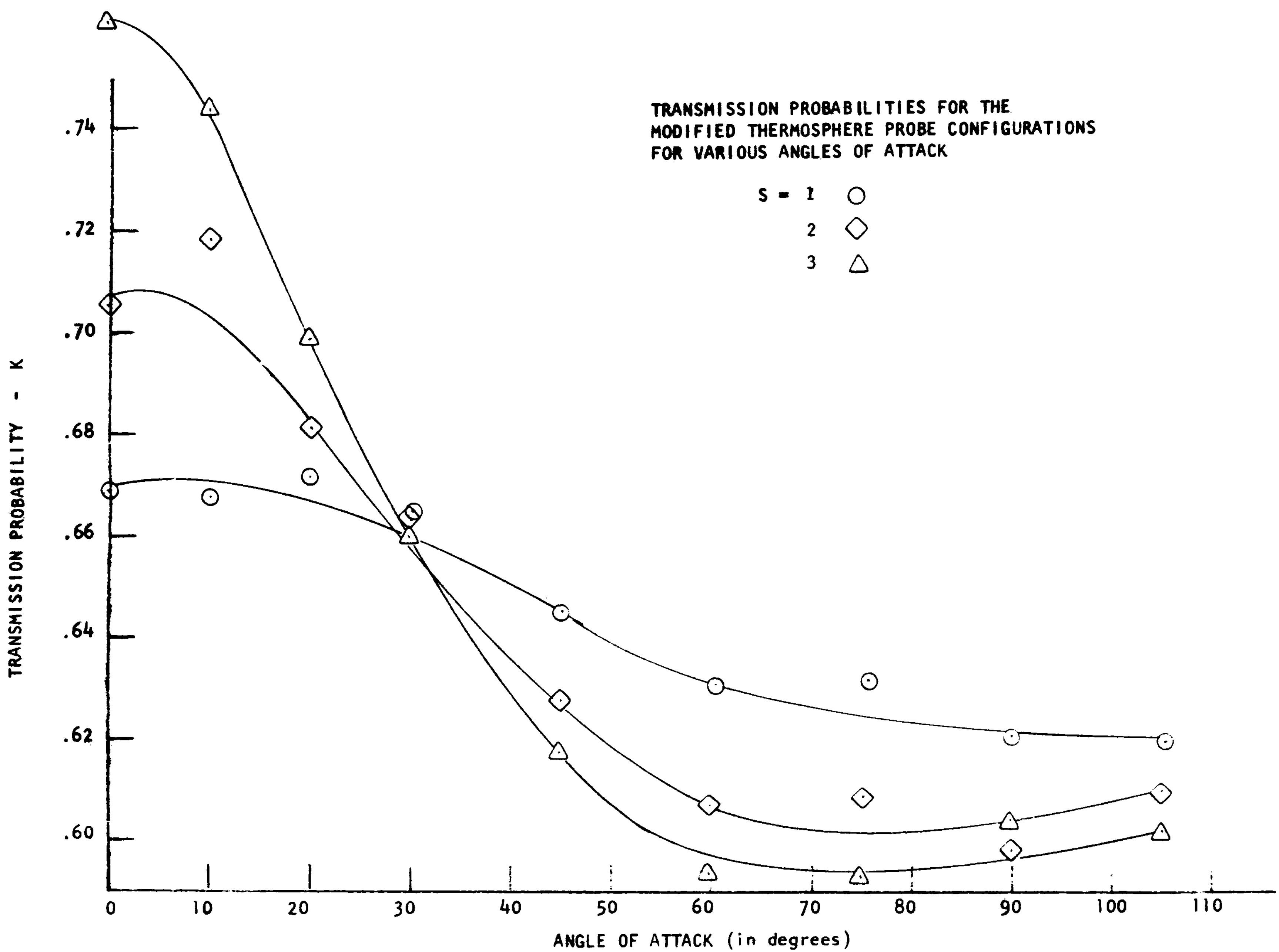
TRANSMISSION PROBABILITIES FOR THE
MODIFIED THERMOSPHERE PROBE CONFIGURATIONS
FOR VARIOUS ANGLES OF ATTACK
S = 1
2
3
TRANSMISSION PROBABILITY - K
.74
.72
.70
.68
.66
.64
.62
.60
0
10
20
30
40
50
60
70
80
90
100
110
ANGLE OF ATTACK (in degrees)

FIGURE 12

APPROXIMATE TIME FOR MOLECULES ENTERING ORIFICE TO REACH THE OMEGATRON SENSOR

Speed ratios = 2.7
Probe velocity = 1739 meters per second
Thermal velocity in tube = 420 meters per second
Diffuse reflections

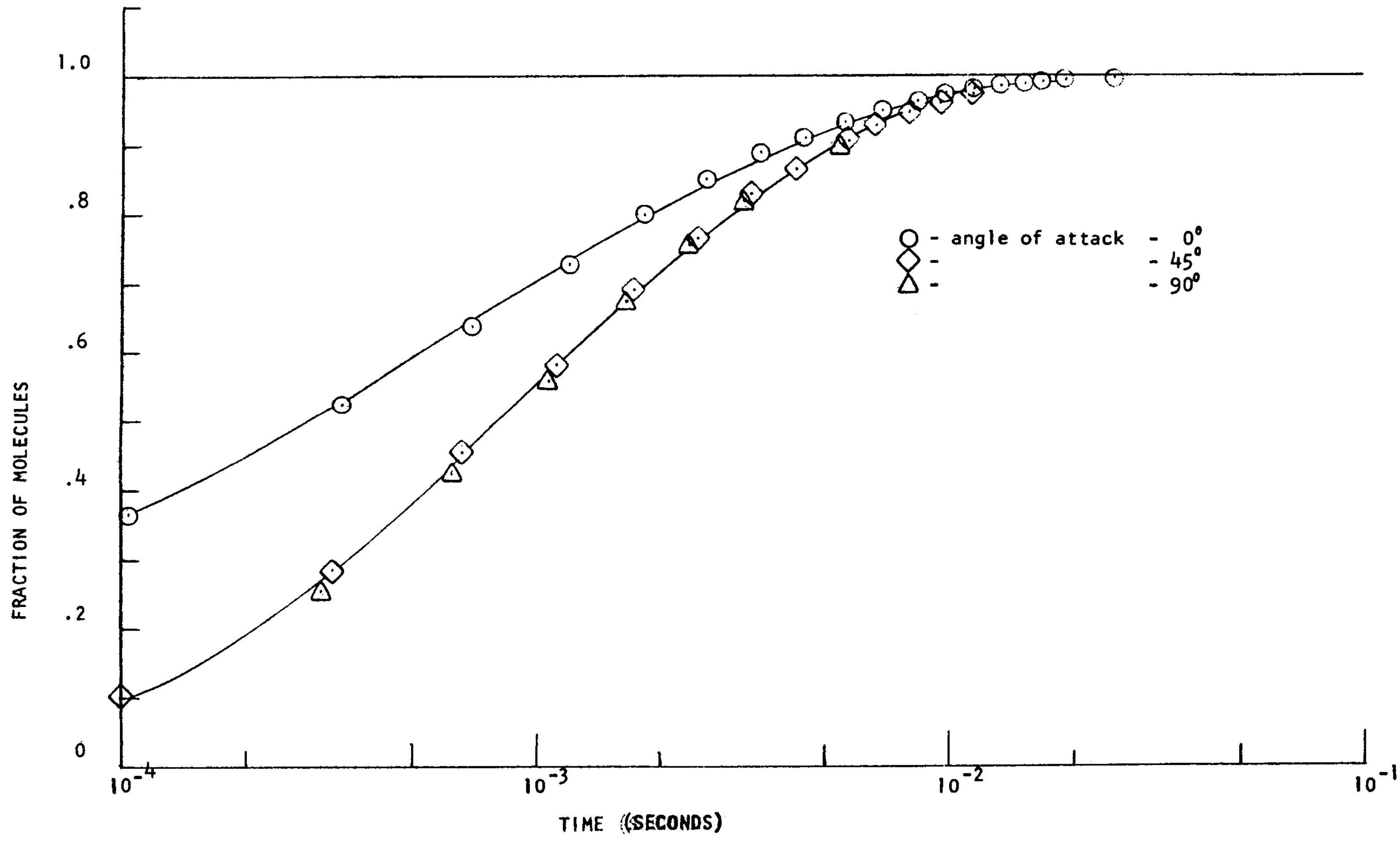

FIGURE 13

RATIO OF MEASURED SIGNAL TO THEORETICAL VALUES FOR NASA PROBE 12.05

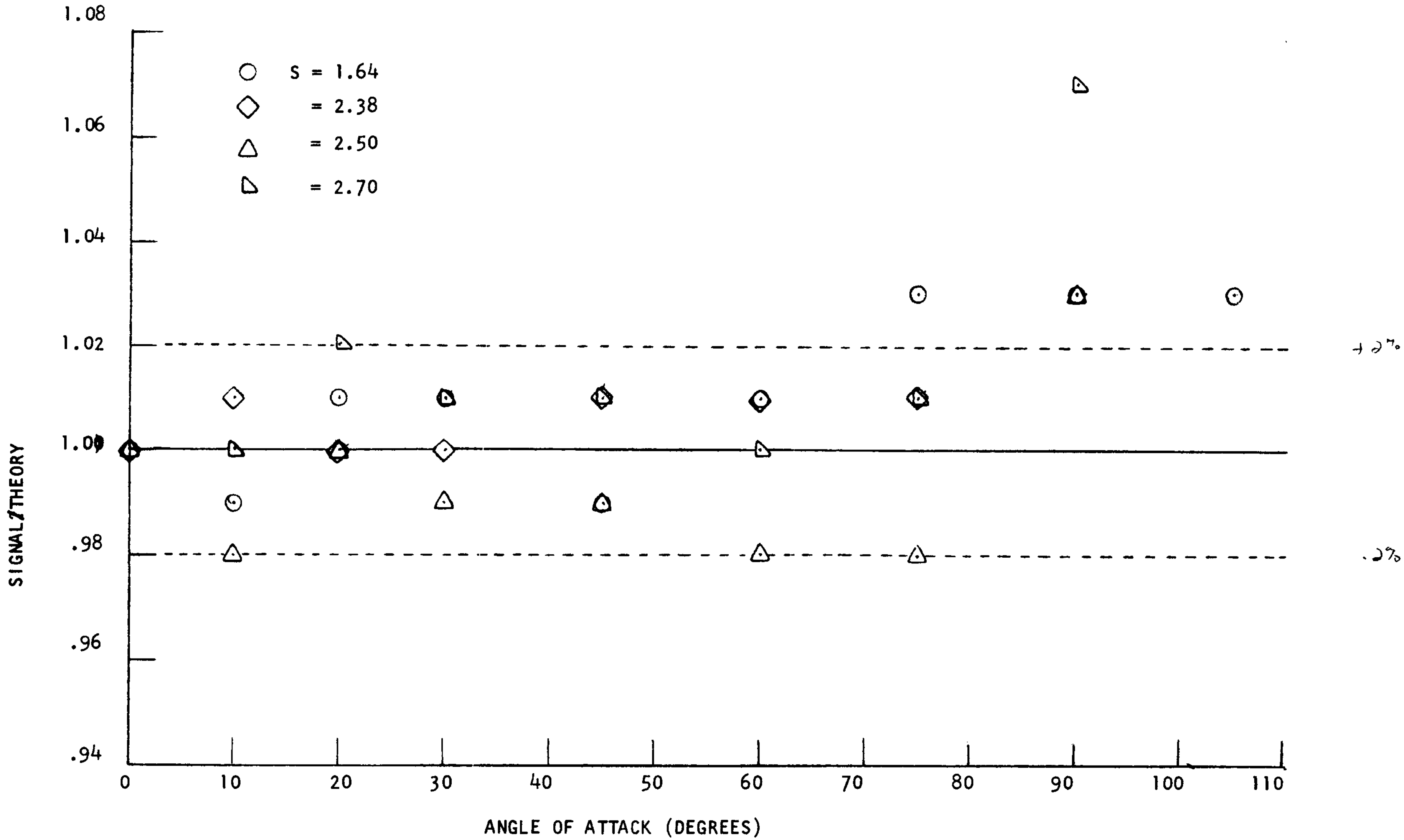

FIGURE 14

APPENDIX A

Response of A Probe in Free Molecule Flow

The response of a probe in free molecule flow is easily shown in the following manner. Consider a cylindrical tube with an orifice (area A_o) at one end opening to the atmosphere and another orifice (area A_i) at the other end, opening to a sensor volume. The number of molecules which enter the orifice (A_o), which pass through the tube, and which exit the tube at the other orifice (A_i) is given by

$$Z_{in} = \frac{N_o \bar{V}_o}{2\sqrt{\pi}} F(S)\, A_o K_o (L/R, S, \alpha),$$

where

Z_{in} = number of molecules entering the sensor volume

N_o = number density of the ambient gas

$\bar{V}_o$ = average speed of the ambient gas molecule

$= \sqrt{\frac{2kT_o}{m}}$

k = Boltzmann's constant

m = mass of a molecule

T_o = temperature of the ambient gas

S = speed ratio = $U \cos \alpha / V_m$

U = mass velocity of the probe relative to the gas

V_m = most probable speed of ambient molecules

α = angle between the normal to the orifice and the velocity vector

$K_o(L/R, S, \alpha)$ = Clausing probability factor in the direction from A_o to A_i

L/R = length to radius ratio of the duct.

The number of molecules in the sensor volume which leave that volume through the orifice (A_i) and return to the atmosphere is given by

$$Z_{out} = \frac{N_s \bar{V}_s}{2} A_i K_i (L/R, 0, 0),$$

where

Z_{out} = number of molecules leaving the sensor volume

N_s = number density of the gas in the sensor volume

V_s = average speed of the molecule in the sensor volume

$= \sqrt{\frac{2kT_s}{m}}$

T_s = temperature of the gas in the sensor volume

$K_i(L/R,0,0)$ = Clausing probability function for the direction from A_i through A_o.

For equilibrium conditions,

$$Z_{in} = Z_{out}.$$

Thus,

$$\frac{N_o \bar{V}_o}{2} F(S)\ A_o K_o (L/R, S, \alpha) = \frac{N_s \bar{V}_s}{2} A_i K_i (L/R, 0, 0).$$

When $S = 0$, $T_o = T_s$ and $N_o = N_s$,

$$A_o K_o (L/R, 0, 0) = A_i K_i (L/R, 0, 0)$$

so that

$$K_i = \frac{A_o}{A_i} K_o (L/R, 0, 0).$$

Thus,

$$N_s = \frac{N_o \bar{V}_o \ F(S) \ K_o(L/R,S,\alpha) \ A_o}{\bar{V}_s \ K_o(L/R,0,0) \ \frac{A_o}{A_i} \ A_i}$$

$$= \frac{N_o \bar{V}_o \ F(S) \ K_o(L/A,S,\alpha)}{\bar{V}_s \ K_o(L/A,0,0)}$$

and

$$\frac{\bar{V}_o}{\bar{V}_s} = \frac{\sqrt{\frac{2kT_o}{m}}}{\sqrt{\frac{2kT_s}{m}}} = \sqrt{T_o/T_s}$$

so that

$$N_s = N_o \sqrt{T_o/T_s} \quad X(S) \ \frac{K_o(L/R,S,\alpha)}{K_o(L/R,0,0)} \ ,$$

or, in terms of pressure, since $N_j = P_j/kT_j$,

$$\frac{P_s}{kT_s} = \frac{P_o}{kT_o} \ \sqrt{T_o/T_s} \ F(S) \ \frac{K_o(L/R,S,\alpha)}{K_o(L/R,0,0)}$$

$$P_s = P_o \sqrt{T_s/T_o} \ F(S) \ \frac{K_o(L/R,S,\alpha)}{K_o(L/R,0,0)} \ .$$

REFERENCES

1. Spencer, N. W., D. R. Taeusch, and G. R. Carignan, "N_2 Temperature and Density Data for the 150 to 350 km Region and Their Implications," Annales De Geophysique, Tome 22, No. 2, Avril-Juin, 1966.

2. Niemann, Hasso B. and B. C. Kennedy, "Omegatron Mass Spectrometer for Partial Pressure Measurements in the Upper Atmosphere," The Review of Scientific Instruments, Volume 37, No. 6, June 1966, p. 722.

APPROVAL NASA TM X-53641

AN ANALYSIS OF THE MOLECULAR KINETICS OF THE THERMOSPHERE PROBE

by James O. Ballance

The information in this report has been reviewed for security classification. Review of any information concerning Department of Defense or Atomic Energy Commission programs has been made by the MSFC Security Classification Officer. This report, in its entirety, has been determined to be unclassified.

This document has also been reviewed and approved for technical accuracy.

W. K. Dahm
Chief, Aerophysics Division

E. D. Geissler
Director, Aero-Astrodynamics Laboratory

DISTRIBUTION

DIR

R-DIR

MS-IL (8)

MS-IP

MS-H

DEP-T

CC-P

I-RM-M

MS-T (6)

R-ASTR
Dr. Haeussermann

R-RP
Dr. Stuhlinger
Mr. Heller
Dr. Shelton

R-AERO
Dr. Geissler
Mr. Jean
Mr. Vaughan
Mr. R. E. Smith
Dr. Heybey
Mr. J. Johnson
Mr. J. Carter
Mr. Baker
Mr. Dahm
Mr. Ballance (40)
Mr. Horn
Mr. Lindberg
Dr. H. Krause
Mr. Thomae

EXTERNAL DISTRIBUTION

Sci. & Tech. Info. Facility (25)
Box 33, NASA Rep. (S-AK/RKT)
College Park, Md.

Langley Research Center
Langley Sta.
Hampton, Va.

Lewis Research Center
21000 Brookpark
Cleveland, Ohio
Attn: Mr. Lloyd Krause
Mr. Edward Richley
Library

Goddard Space Flight Center
Greenbelt, Md.
Attn: Mr. George Newton
N. W. Spencer
Library

JPL
4800 Oak Grove Dr.
Pasadena, California

Ames Research Center
Moffett Field, California

Manned Spacecraft Center
Houston, Texas
Attn: Library

Arthur D. Little, Inc.
Cambridge, Mass.

Northrop Space Laboratories
Huntsville, Alabama

AEDC
Arnold Air Force Station, Tenn.

EXTERNAL DISTRIBUTION (Continued)

ARO, Inc.
AEDC
Arnold Air Force Station, Tenn.
Attn: Library

Univ. of Ill.
Urbana, Ill.

Mass. Inst. of Tech.
Cambridge, Massachusetts
Attn: Dr. Robert Stickney
Dr. L. Trilling

Celestial Research Corp.
1015 Fremont Ave.
South Pasadena, Calif.
Attn: Dr. Raymond Chuan
Mr. John Wainwright
Mr. Don Wallace

Univ. of Ala.
University, Ala.
Attn: Dr. Walter Schaetzle

Ga. Inst. of Tech.
Atlanta, Georgia
Attn: Dr. A. B. Huang

Inst. of Aerophysics
University of Toronto
Toronto, Canada
Attn: P. C. Hughes
Dr. G. N. Patterson

Cornell Aeronautical Lab., Inc.
Buffalo, New York

McDonnell Aircraft Corp.
P. O. Box 516
Attn: E. S. J. Wang
St. Louis, Missouri

Univ. of Calif.
Radiation Laboratory
Livermore, California

Lockheed Aircraft Corp.
Huntsville, Ala.
Attn: Dr. C. Fan
Mr. J. Robertson
Mr. A. Shirley
Library

Brown Engineering Co.
Huntsville, Ala.
Attn: Library

Heat Technology Lab.
Huntsville, Alabama

Univ. of Mich.
Ann Arbor, Mich.
Attn: Dr. A. G. Hansen
George Carignan(5)
Hasso Niemann (5)
David Tausch (5)
Library